CHAPTER V

PARTICLE VELOCITY DISTRIBUTION IN TWO-PHASE AND THREE-PHASE FLUIDIZED BED

5.1 Introduction

A number of researchers have investigated the movement of particles in the fluidized bed. Chen and Fan (1992) used PIV system (Particle Image Velocimetry) to characterize the flow structure in a three-dimensional Gas-Liquid-Solid fluidized bed. Carlos and Richardson (1968) measured particles velocities in a liquid-solid fluidized bed. The measurements were done by photographing the movement of tracer particles inside the bed, where dimethyl phthalate was used as liquid, glass beads with 0.8 cm in diameter as solids, and darkened glass beads with the same diameter as tracer particles. The liquid had the same refractive index as the particles. Hence, only the darkened particles were visible. They demonstrated that the velocity distribution follows an approximately Maxwellian distribution about its mean.

Recently, Devanathan et al. (1990) monitored the motion of a single neutrally buoyant radioactive particle by an array of scintillation detectors in an air-water system, and measured the time and ensemble averaged tracer particle velocities. They adopted this technique, called Computer Average Radio-active Particle Tracing (CARPT), to obtain time and volume averaged liquid flow fields in a bubble column.

The objective of this experimental investigation was to conduct well-defined fluidized bed experiments to measure the instantaneous particle velocities. It would also

provide useful data for distinguishing between the distribution function for velocity fluctuations and the Maxwellian distribution. The data provided by the experiments are particles velocities components in the axial and radial directions, and the bubble sizes. Experiments were conducted in a two-dimensional fluidized bed made of transparent acrylic (plexiglas) with a uniform air distributor and also in a two-dimensional fluidized bed with a central jet.

In this chapter, a direct imaging technique is used to measure the instantaneous velocity or velocity distribution in both the gas-liquid-solid fluidized bed as well as the liquid-solid fluidized bed experiments. The effects of gas and liquid flow rates and particle concentration on macroscopic flow behavior including particles movement, bubble size and liquid-solid circulation were examined. From these experimental data, the values for granular temperature and solids viscosity were computed, as described by Gidaspow (1994). The computed solid viscosity was in agreement with the experimentally measured solids viscosity, described in detail in the Chapter 6.

5.2 Apparatus and Experimental Procedure

The apparatus for the velocity measurements consists of essentially two units: a high resolution micro-imaging / measuring system and a fluidized bed. In this study, the experimental studies were carried out in two different types of fluidized beds, namely, a two-dimensional fluidized bed with a uniform distributor and a two-dimensional fluidized bed with central jet. The experimental apparatus is shown schematically in Figures 5.1 and 5.2.

5.2.1 High Resolution Micro-Imaging / Measuring System. This system comprises two units :

1) SONY high resolution color CCD video camera equipped with electronic shutter speed settings ranging from OFF to 1/10000 sec and SONY super fine pitch color monitor, and

2) A 486 / 33 MHz IBM compatible personal computer with a Micro-Imaging Board inside and a Micro-Imaging software, Image-Pro Plus.

5.2.2 Fluidized Bed with Uniform Distributor. Figure 5.1 shows a two-dimensional acrylic (plexiglas) rectangular fluidized bed with a height of 213.36 cm, width of 30.48 cm, depth (thickness) of 5.08 cm, and with a uniform gas distributor. The ballotini (leaded glass beads) particles, with 800 μm in diameter and a density of 2.94 g/cm^3, are fluidized inside the bed by means of water and air. Water from a fifty-five gallon storage tank is introduced into the bed from the bottom through a rotameter by means of a centrifugal pump. Air from a compressor enters through a distributor section consisting of six porous tubes with a nominal pore diameter of 41.88 μm and a perforated plate. These six staggered tubes are located below the perforated plate. The distributor section is located at 50 cm (height) in the bed.

5.2.3 Fluidized Bed with Central Jet. Figure 5.2 shows a two-dimensional acrylic (plexiglas) rectangular fluidized bed with a height of 233.7 cm, width of 48.3 cm, depth of 2.54 cm, and with a central jet. The particles used in this fluidized bed were glass beads with a 1 mm diameter and a density of 2.55 g/cm^3. Water is fed to the bed in the same way as that in the previous bed. The air from the compressor enters the bed

through three separate rotameters. Two rotameters are connected to the left bottom and the right bottom inlets of the bed. The third rotameter is connected to the central bottom inlet of the bed, which is used as a central jet inlet, and is located right below the distributor section. The distributor section consists of one perforated plate with many 0.08 cm diameter holes and is located at 50 cm from the bottom of the bed.

5.2.3 Experimental Procedure. The gas and liquid were injected inside the fluidized bed at several different velocities. These velocities are reported in the graphs. As the gas and liquid entered the bed through the distributor section, the particles were fluidized. Both the gas and liquid exited from the top of the bed, and were directed through three 1 inch (2.54 cm) diameter openings back to the fifty gallon storage tank, where the gas was separated from the liquid.

In order to get a good visualization of microscopic movement of particles, a fiber-optic light was reflected on the field of view in the front and the back of the bed. The field of view in most experiments was a 2 cm x 2 cm area. As the particles were fluidized inside the bed, the camera with a zoom lens with a range of 18-108 mm and close up focus transferred its field of view to the monitor with streak lines. These streak lines represented the distance traveled by the particles in a given time interval specified on the camera. The images were then captured and digitized by a micro-imaging board and analyzed using Image-Pro Plus software. Measurements were conducted at several different radial and axial locations (see Figure 5.3).

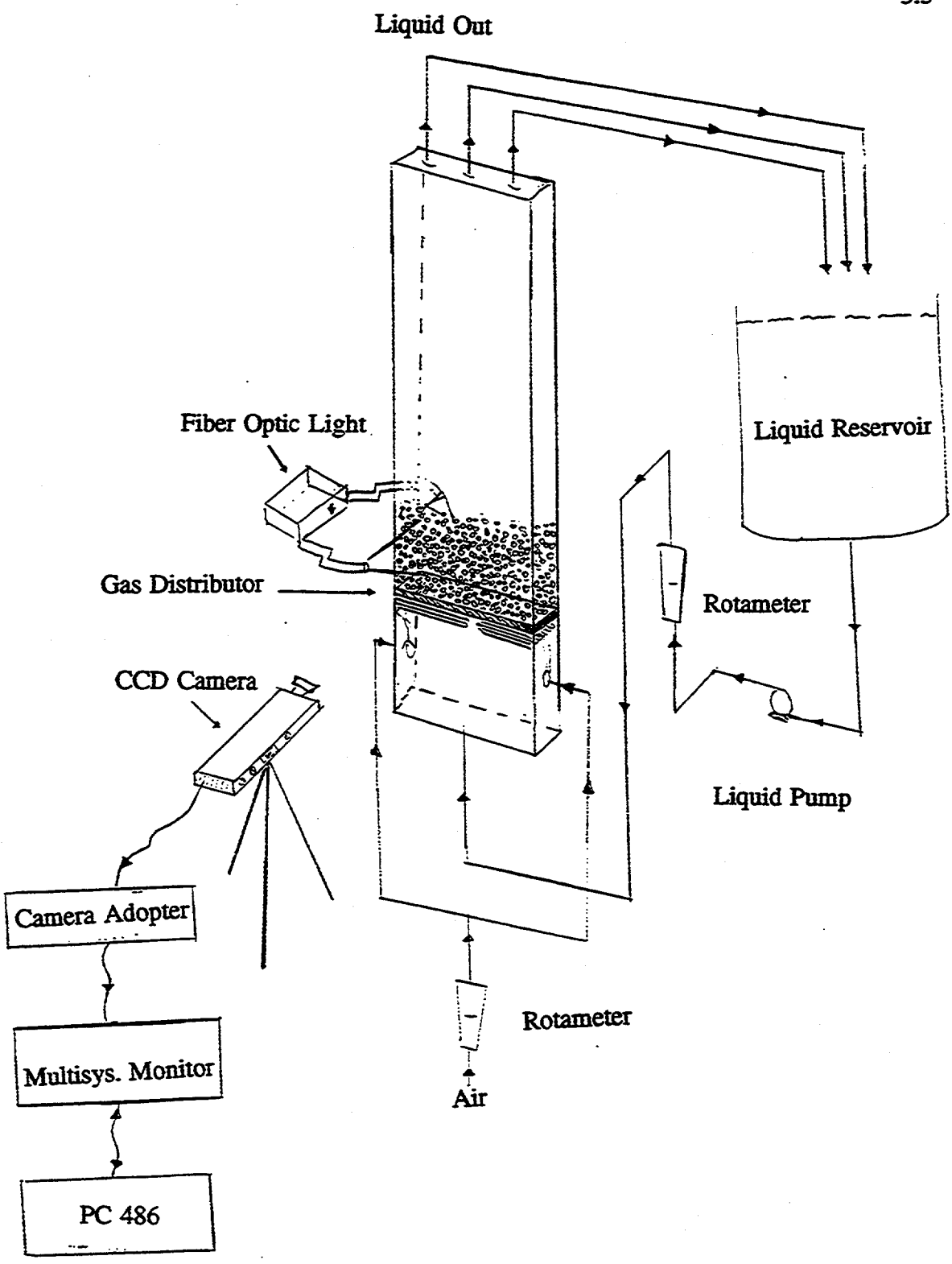

Figure 5.1. Schematic Diagram of Experimental Apparatus of Fluidized Bed W/uniform Distributor

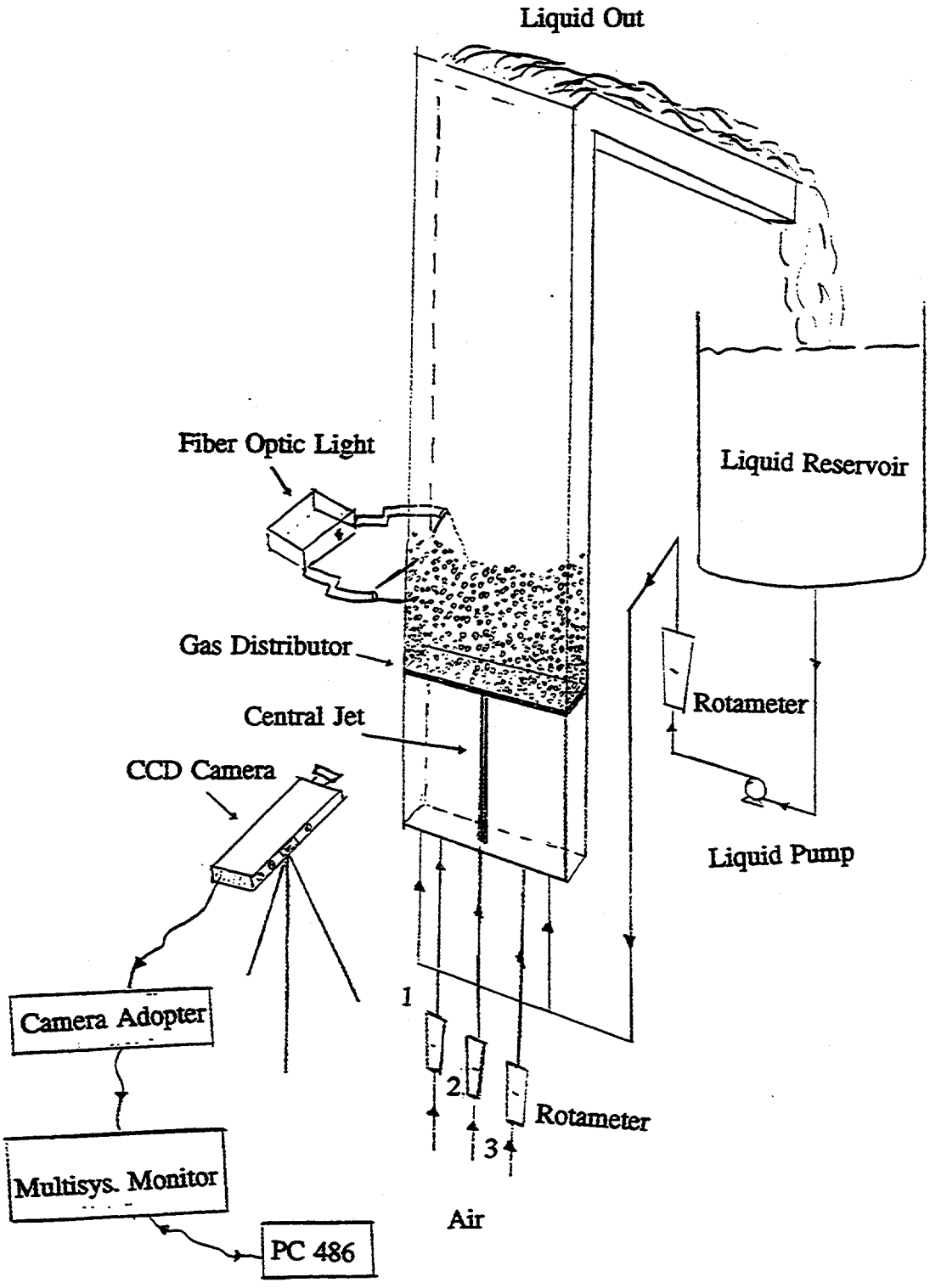

Figure 5.2. Schematic Diagram of Experimental Apparatus of Fluidized Bed W/central Jet Distributor

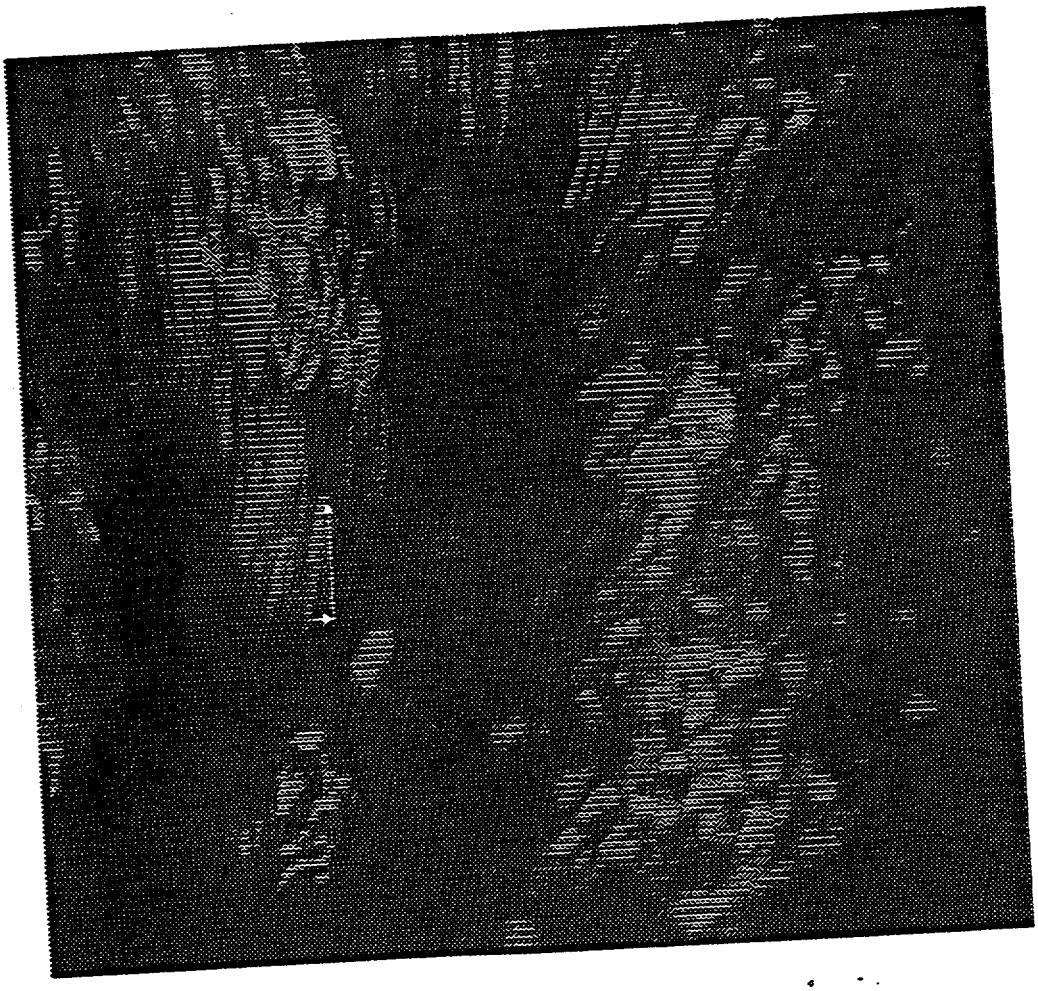

Figure 5.3. The Image Captured by the Recording System

5.3 Analysis of Results

In this investigation, the computer recorded the distances traveled by the particles in both -x and -y directions. Using these data, instantaneous particles speed, axial and radial velocities, their variances, mean axial and radial velocities, and standard deviations were calculated. Also, the experimental velocity distribution was examined and analyzed with these set of data.

The experiments were conducted in two parts, (a) with a liquid-solid fluidized bed, and (b) with a gas-liquid-solid fluidized bed. In the gas-liquid-solid fluidized bed experiments, two different designs, (i) with uniform distributor, and (ii) with central jet were studied.

5.3.1 Liquid-Solid Fluidized Bed Experiment. Figures 5.4, 5.5 and 5.6 show typical experimental data that are plotted for the distribution function, f, as a function of instantaneous particles speed, axial velocity and radial velocity, respectively. Figure 5.7 also shows frequency plot for solids speed at different locations. The frequency, f, expressed as the fraction of the total number of velocities falling in the interval, divided by the size of the interval and the values for velocities were made of the mean value of 120 data at each position. As seen in Figures 5.4 to 5.7, the velocity fluctuations follow normal distribution. The normal distribution for solids fluctuating velocities, also called Maxwellian distribution, can be written as follows (Gidaspow,1994):

$$f(c_y) = \frac{1}{\sqrt{2\pi\sigma^2}} \exp\left(-\frac{(c_y - v_y)^2}{2\sigma^2}\right) \qquad (5.1)$$

where σ^2 is variance and is equal to the granular temperature Θ, c_y and v_y are the

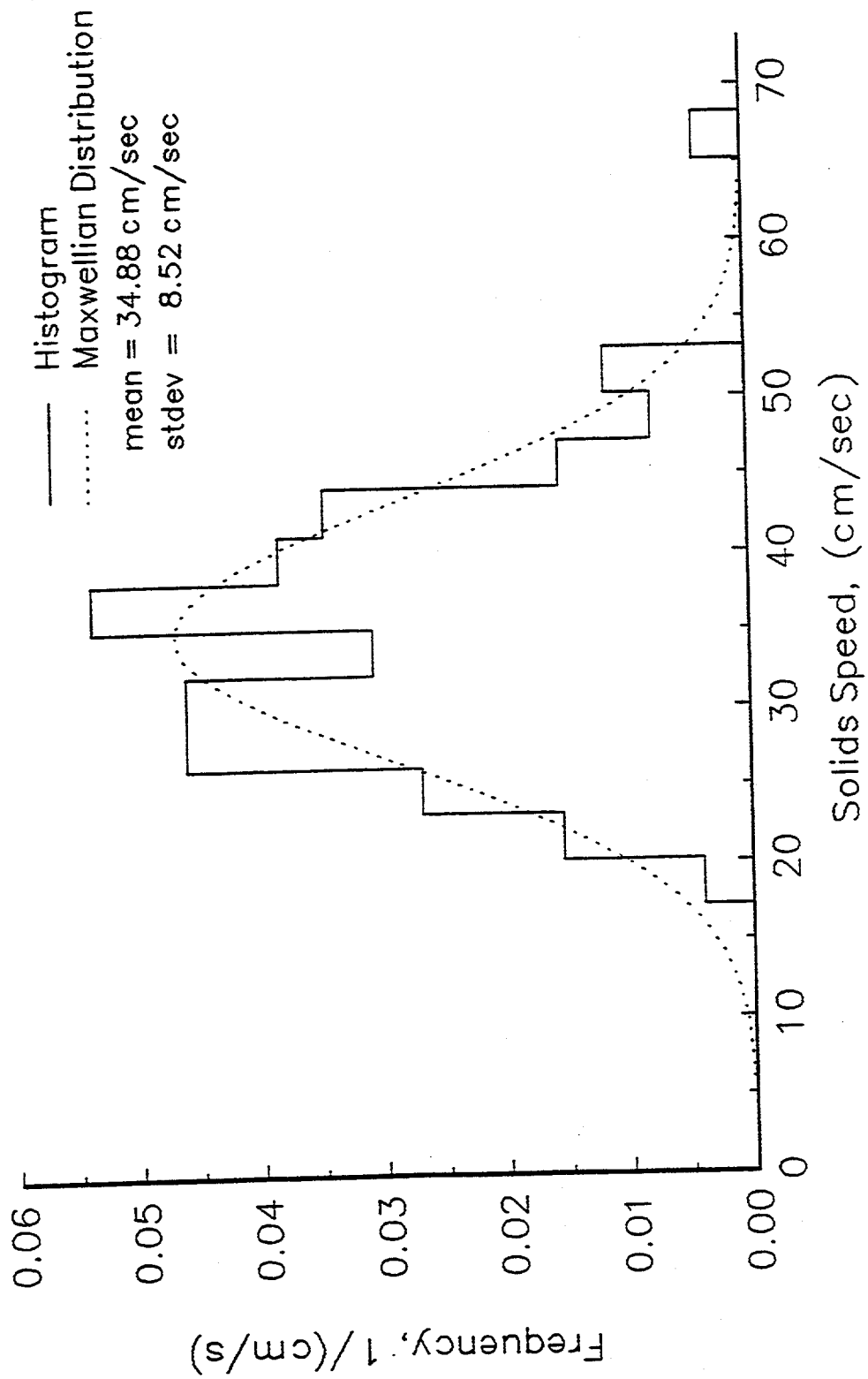

Figure 5.4. Distribution of Mean Solid Speed at X=4 cm and Y=4.5 cm for Liquid-Solid System with V_l=4 cm/sec

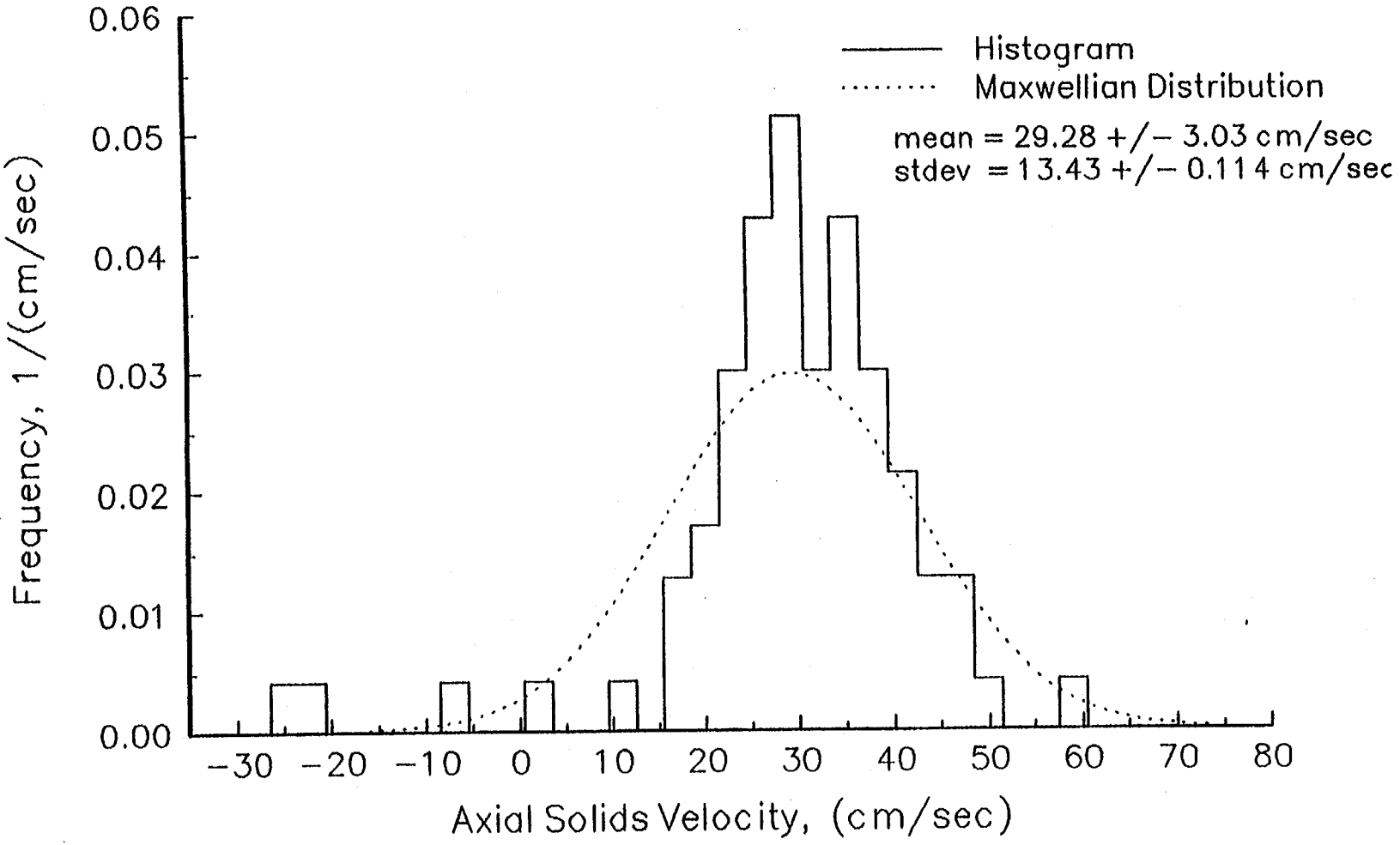

Figure 5.5. Distribution of Axial Velocity of Particles at X=4 cm and Y=4.5 cm for Liquid-Solid System with V_t=4 cm/sec

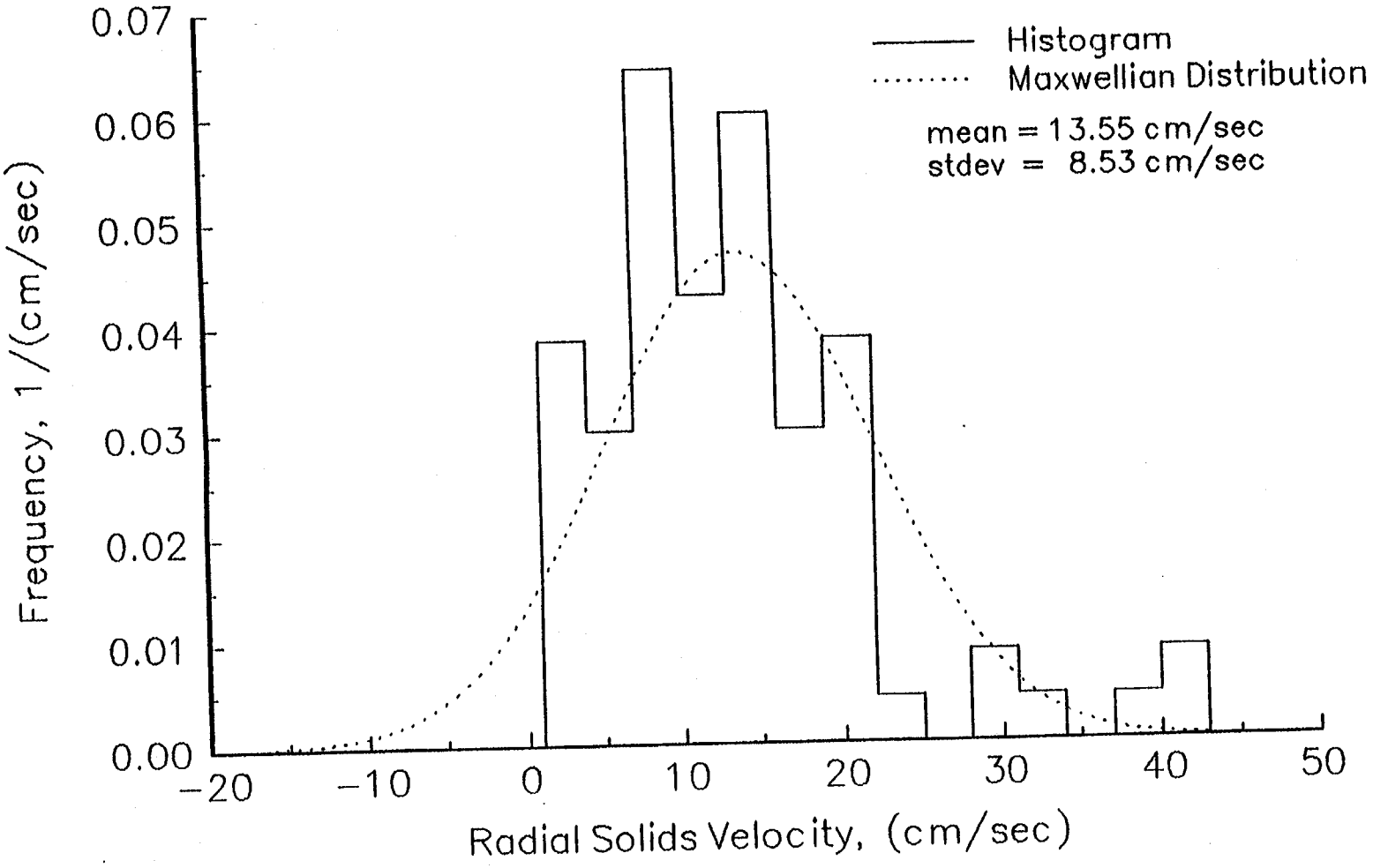

Figure 5.6. Distribution of Radial Velocity of Particles at X=4 cm and Y=4.5 cm for Liquid-Solid System with V_t=4 cm/sec

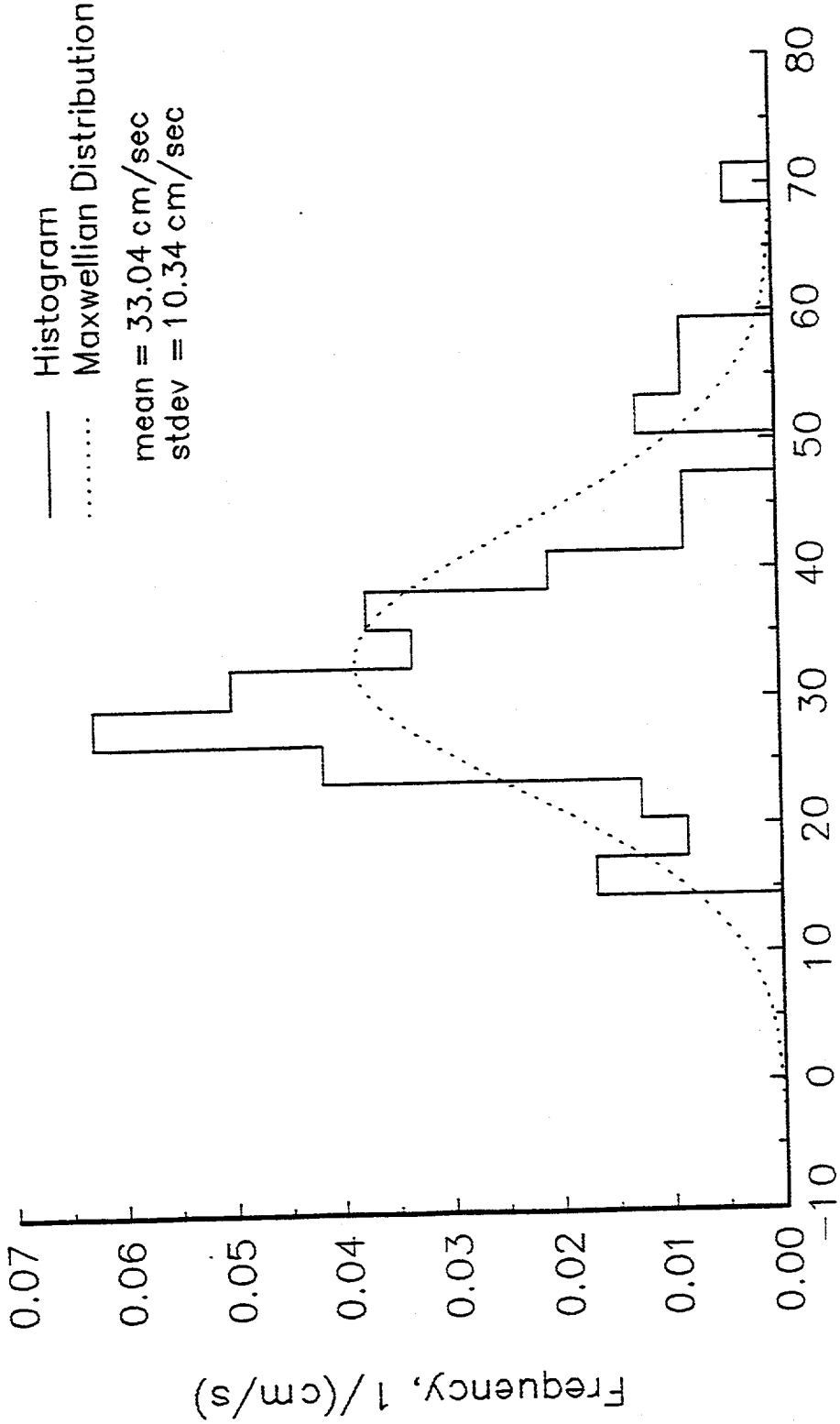

Figure 5.7. Distribution of Mean Solid Speed at X=4 cm and Y=4.5 cm for Liquid-Solid System with V_l=6 cm/sec

particles velocity and mean particle fluctuations in the axial (-y) direction. Similarly, equation (5.1) can also be written for the velocity fluctuations in -x and -z directions.

Figure 5.8 corresponds to the data which were taken by Carlos and Richardson (1968). However, even taking into account that in their experiment, the overall mean particle velocities are zero, the agreement between Figures 5.4 to 5.7 with Figure 5.8, and the Maxwellian distribution is reasonably close. Figures 5.5 and 5.6 clearly show that the two phase (liquid-solid) fluidized bed is anisotropic, and the axial velocity fluctuations greatly exceed the radial velocity fluctuations.

The effect of liquid velocity on particles velocity is plotted in Figure 5.9. Figure 5.9 shows that at higher liquid velocities, more oscillation and collision between the particles occur and, as a result, the granular temperature is higher. Figure 5.10 shows the solid viscosity calculated from granular temperature using equations (7.2) to (7.4). As expected, the calculated solids viscosity increases as the solid volume fraction increases.

5.3.2 Gas-Liquid-Solid Fluidized Bed Experiment. In order to study the effects of the gas flow on the particles velocity, the experiments were performed in the following two beds : fluidized bed with uniform gas distributer, and fluidized bed with central jet.

5.3.2.1 Fluidized Bed with Uniform Distributor. The frequency plots for solids speed, and axial and radial velocities are shown in Figures 5.11, 5.12, and 5.13, respectively. The difference between these measurements and those shown in Figures 5.4 to 5.6 for two-phase fluidized bed experiments was the presence of the gas flow. Figures 5.11 to 5.13 clearly show that in three-phase fluidized bed the velocity fluctuation

distributions are also a Maxwellian distribution.

Figure 5.14 shows speed fluctuation distribution for the same gas and liquid velocity as in Figure 5.11, but at a different location. Figure 5.15 represents the speed fluctuation distribution for the same location as in Figure 5.15, but at a higher liquid flow rate. These figures clearly demonstrate that the velocity fluctuation in two and three-phase fluidized beds follow a Maxwellian distribution. Hence, the basic assumptions used to derive the Kinetic theory of granular solids applys to a fluidized bed.

Figure 5.16 shows the axial velocity profile as a function of radial distance at three different bed heights. It can be seen that the velocities near the wall are moving in a downward direction and far from the wall there are higher peaks. These peaks are due to the bubbles path. These velocity profiles are also observed visually.

The two-dimensional fluidized bed used in the experiment allows flow predominantly in two directions, namely axial (-y) and radial (-x). Hence, the instantaneous velocities measurements were made in the axial-radial (x-y) plane only. However, the -z direction also has a non-zero component of particles fluctuations because of a finite bed depth. Due to the method of selecting the steak lines for measurement it is reasonable to assume that the $< c_z^2 > = < c_x^2 >$, and that both the -z and -x directions have zero mean gas and liquid velocities. Thus, the velocities fluctuations can be written as:

$$\begin{aligned} \langle C^2 \rangle &= \langle C_x^2 \rangle + \langle C_y^2 \rangle + \langle C_z^2 \rangle \\ &= 2 \langle C_x^2 \rangle + \langle C_y^2 \rangle \end{aligned} \qquad (5.2)$$

where $< c_x^2 >$, and $< c_y^2 >$ are the measured mean square velocity fluctuations in -x and -

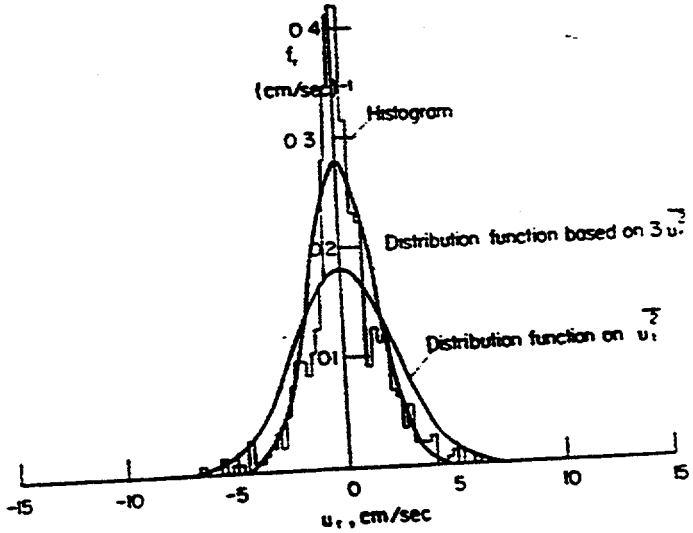

Histogram of radial velocities.

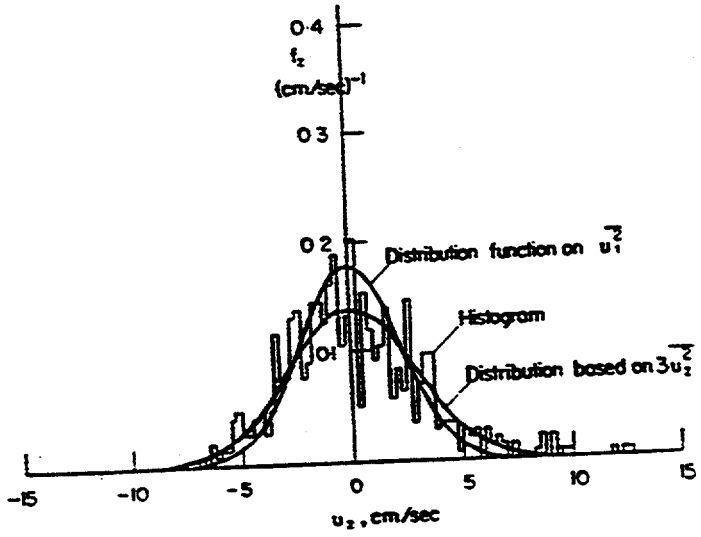

Histogram of axial velocities.

Figure 5.8. Velocity Distribution of Particles (Carlos, and Richardson, 1968)

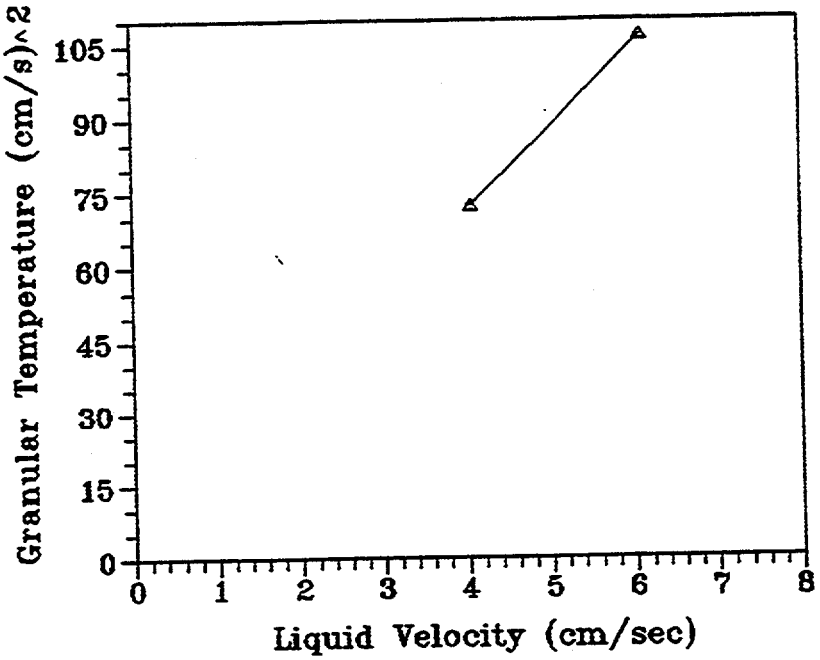

Figure 5.9. Solids Granular Temperature as Function of Liquid Velocity at X=4 cm, and Y=4.5 cm

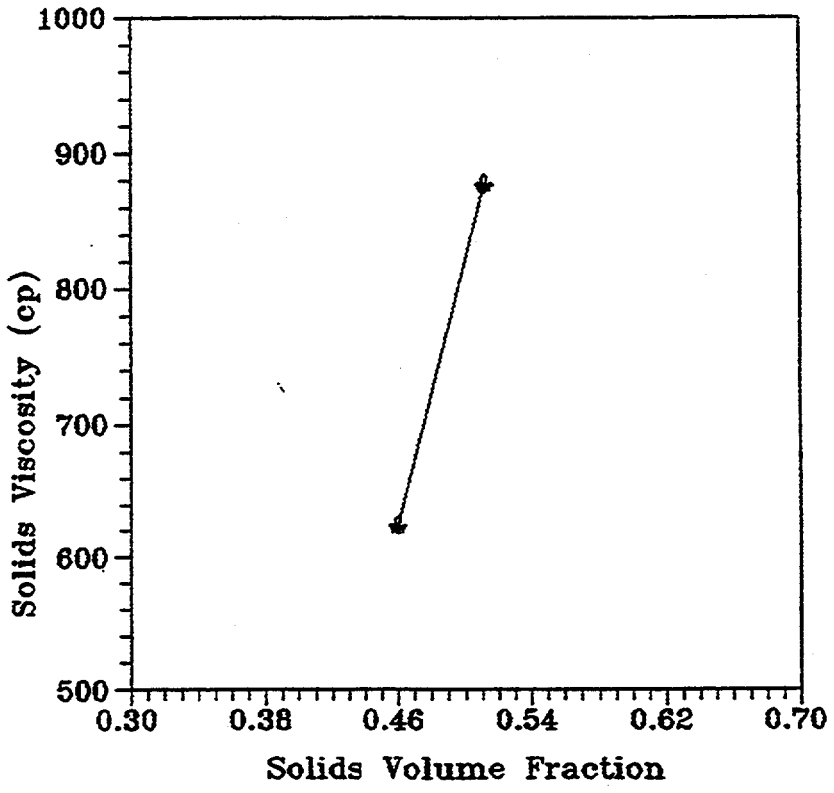

Figure 5.10. Solids Viscosity As Function of Liquid Velocity in Liquid-Solid Fluidized Bed

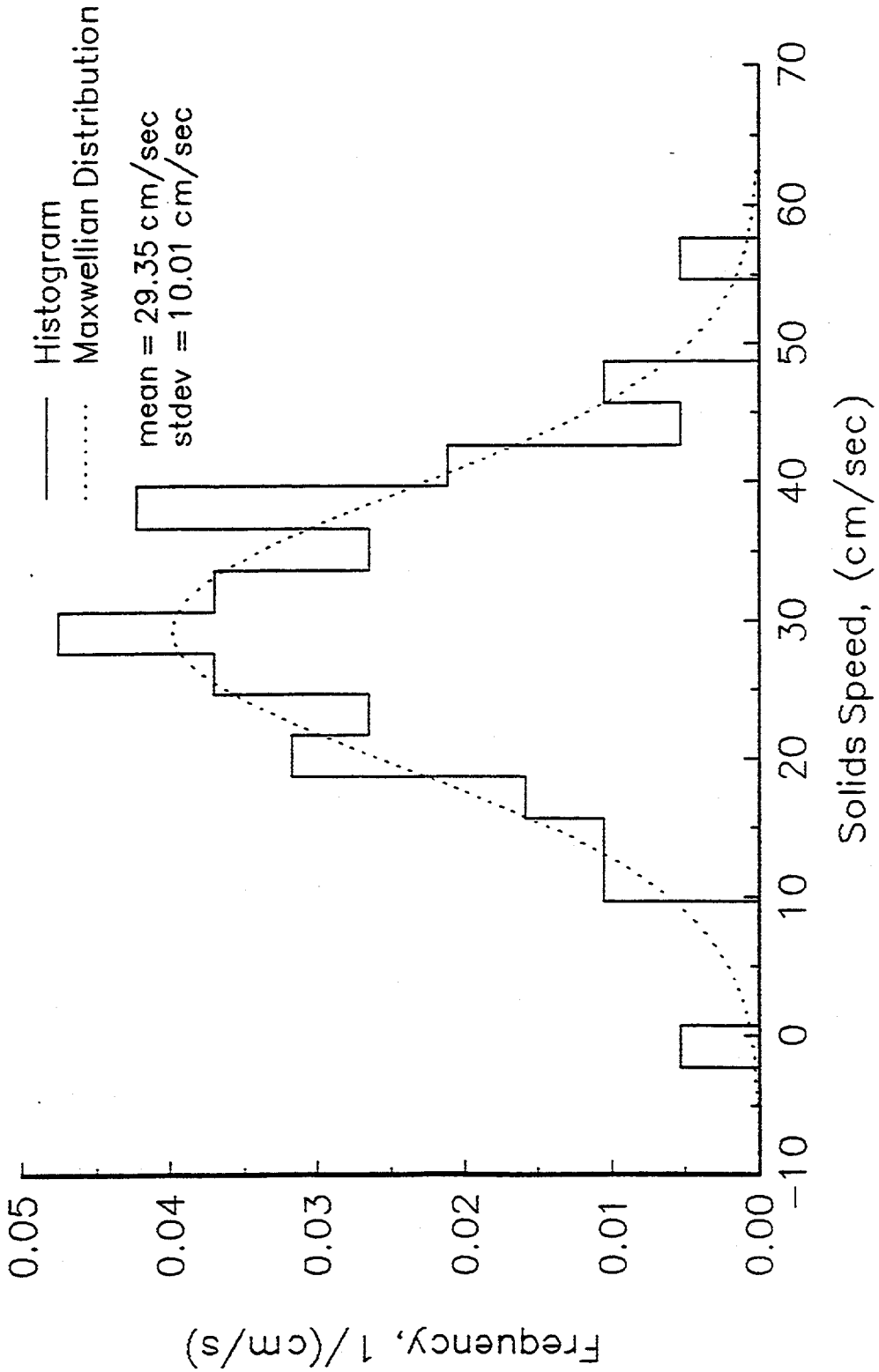

Figure 5.11. Distribution of Mean Solid Speed at X=4 cm and Y=4.5 cm for Liquid-Solid-Gas System with V_l=4 cm/sec and V_g=3.36 cm/sec

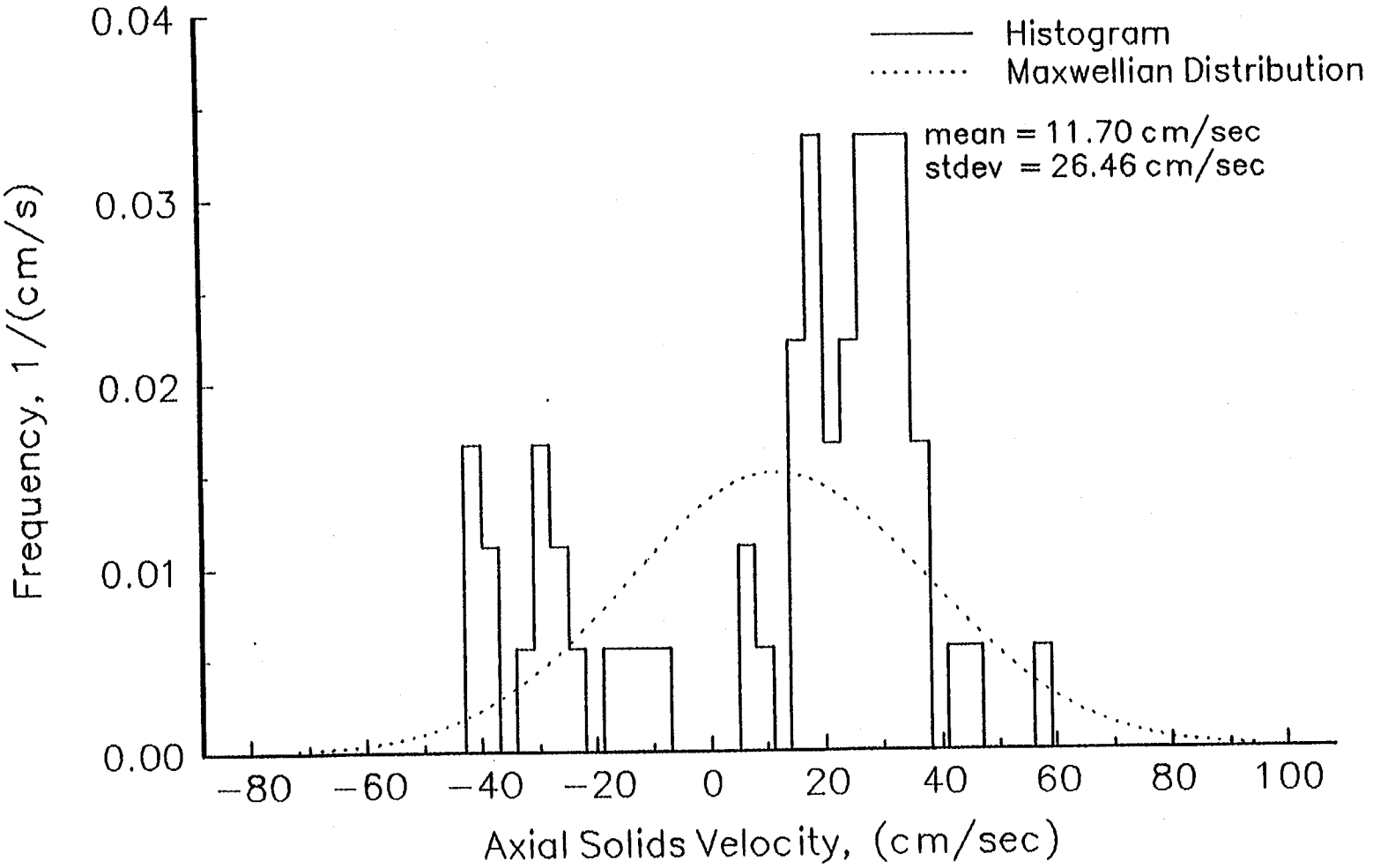

Figure 5.12. Distribution of Axial Velocity of Particles at X=4 cm and Y=4.5 cm for Liquid-Solid-Gas System with V_l=4 cm/sec and V_g=3.36 cm/sec

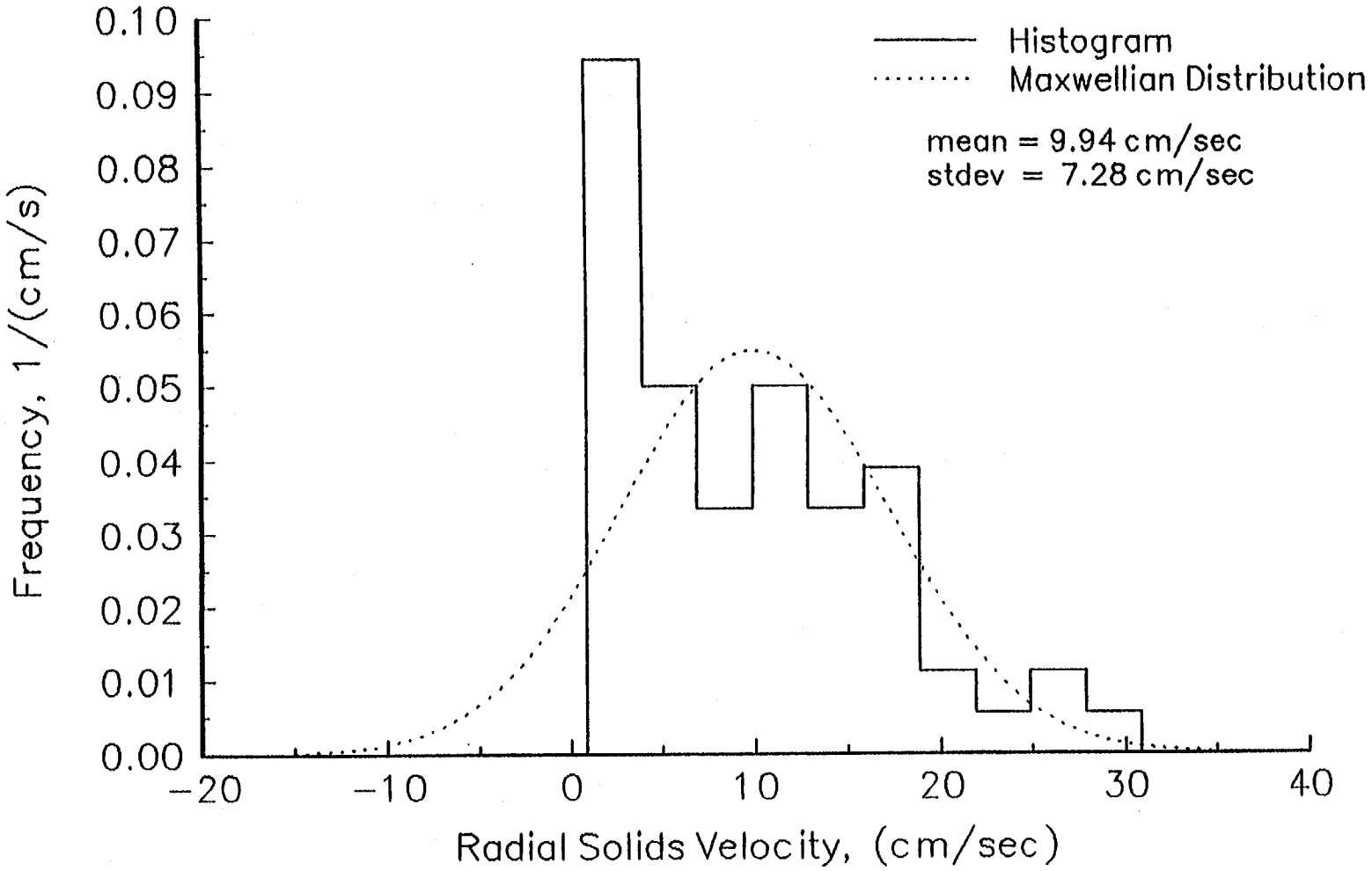

Figure 5.13. Distribution of Radial Velocity of Particles at X=4 cm and Y=4.5 cm for Liquid-Solid-Gas System with V_l=4 cm/sec and V_g=3.36 cm/sec

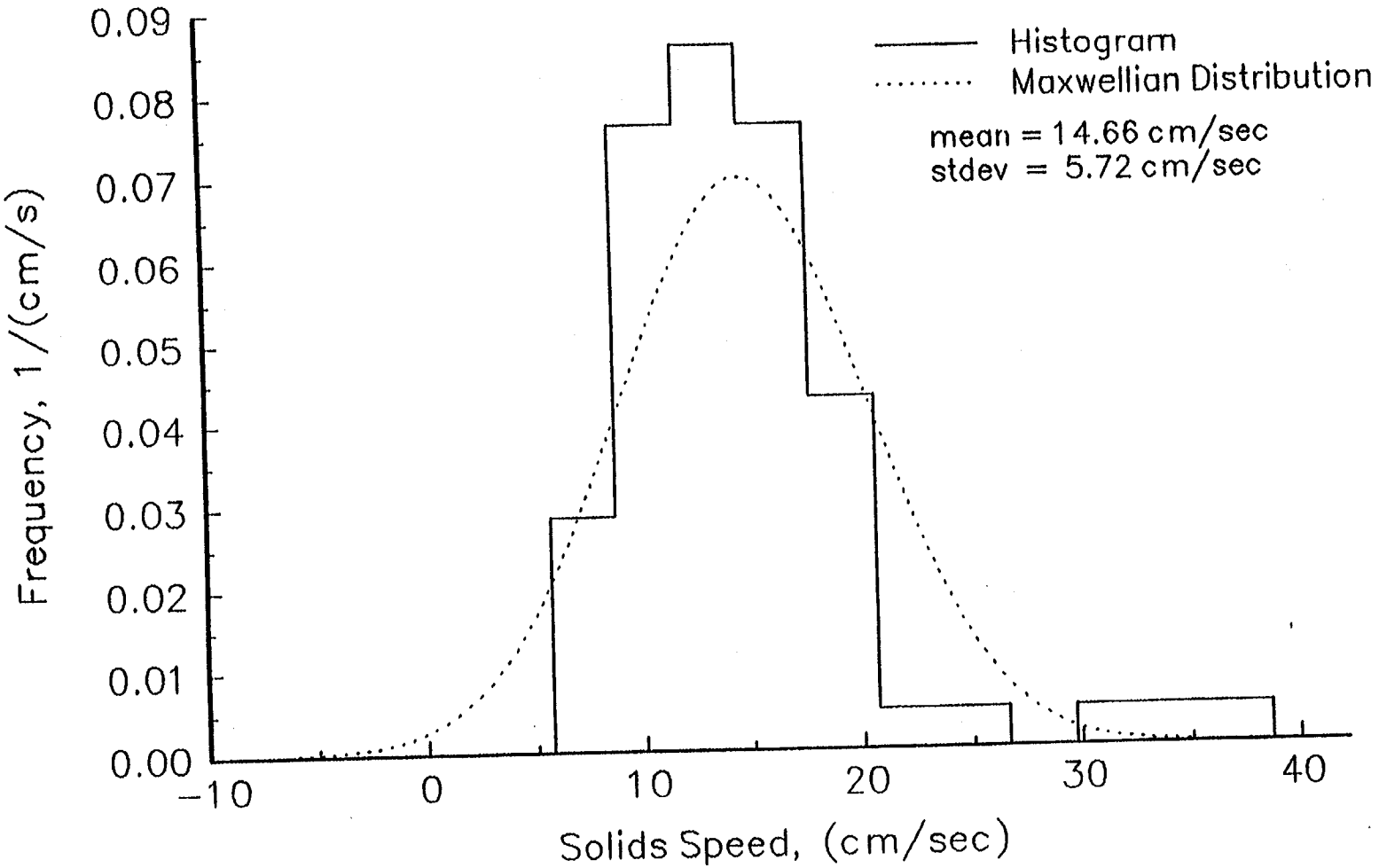

Figure 5.14. Distribution of Mean Solid Speed at X=7.5 cm and Y=9.0 cm for Liquid-Solid-Gas System with V_l=4 cm/sec and V_g=3.36 cm/sec

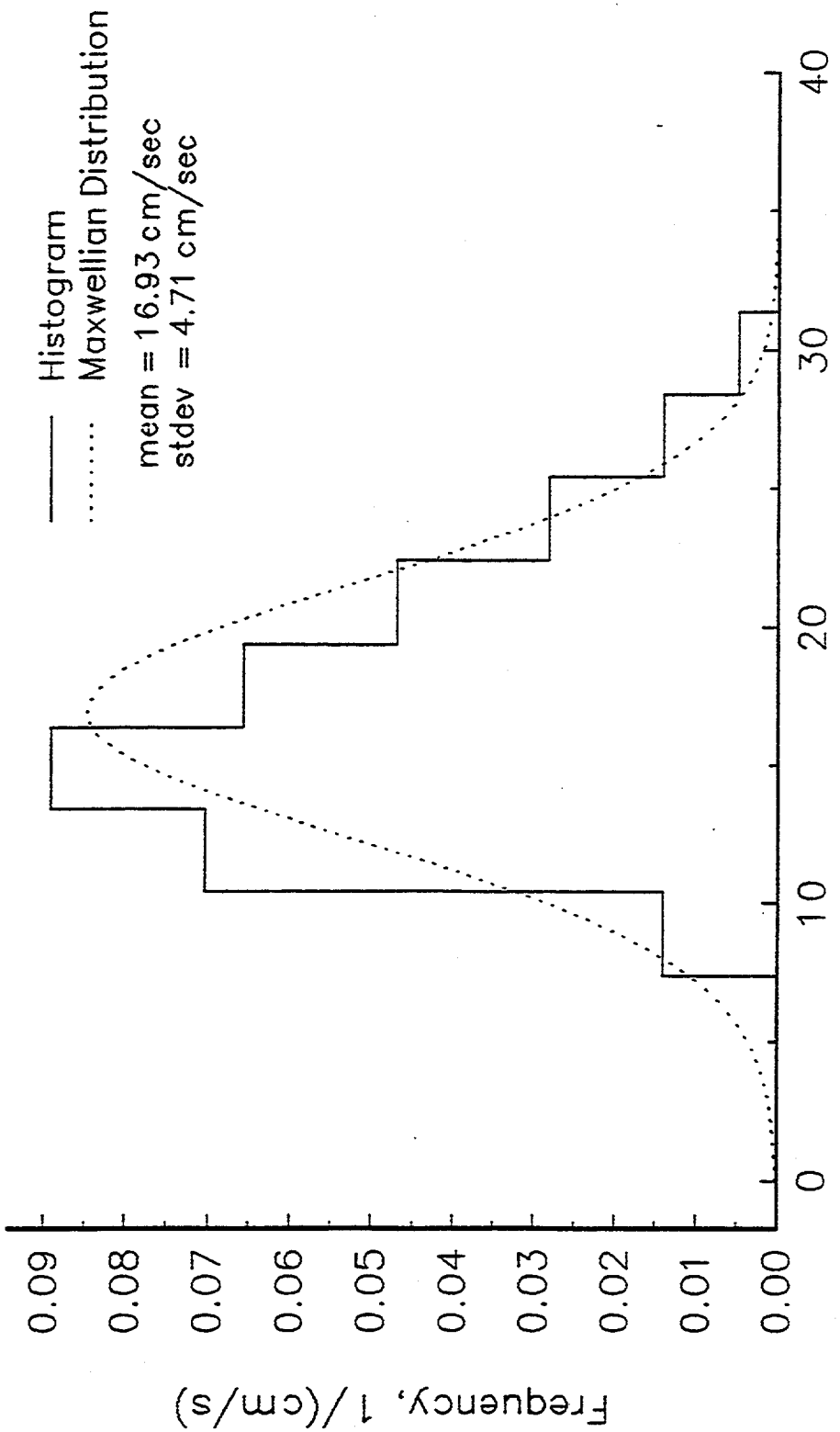

Figure 5.15. Distribution of Mean Solid Speed at X=7.5 cm and Y=9.0 cm for Liquid-Solid-Gas System with V_l=7.23 cm/sec and V_g=3.36 cm/sec

y directions, respectively.

The expression for granular temperature in these experiments can be written as,

$$\Theta = \frac{1}{3} \langle c^2 \rangle = \frac{2}{3} \langle c_x^2 \rangle + \frac{1}{3} \langle c_y^2 \rangle \qquad (5.3)$$

In Figures 5.17 to 5.19 granular temperature is plotted versus width of the bed at three different heights. It is clear that granular temperature is at a maximum value near the center at the bottom of the bed where the measurement for viscosity was also obtained by Brookfield viscometer (see chapter 6).

5.3.2.2 Fluidized Bed with Central Jet. Figures 5.20, 5.21 and 5.22 represent solids speed, axial and radial velocities distribution in the fluidized bed with the central jet. The measurements for these figures were obtained close to the center of the bed. Although in a fluidized bed with a central jet there is a lot of disturbance on the movement of particles, by comparing the figures from the previous section with the figures in this section, one can easily conclude that in both fluidized beds the velocity distribution is Maxwellian. In Figure 5.23, the solid viscosity is increasing with solid volume fraction, very similar behavior was also observed in the fluidized bed with a uniform distributor.

5.4 Conclusion

1. The computed solid viscosity is in agreement with the experimental data from the measured solids viscosity data from experiment (see Chapter 6).

2. The velocity distribution almost every where in the bed and in all types of gas

and liquid flow rate is Maxwellian distribution.

3. The velocity distribution is a Maxwellian distribution in liquid-solid fluidized bed as well as in gas-liquid-solid fluidized bed.

4. The velocity distribution is Maxwellian in both three-phase fluidized beds : fluidized bed with a uniform distributor, and fluidized bed with central jet.

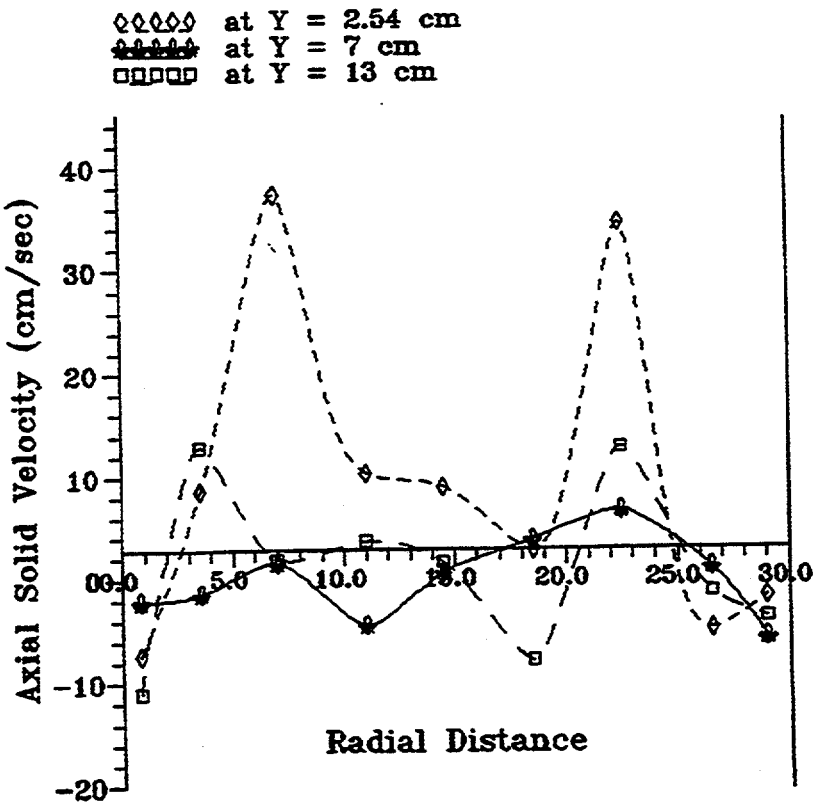

Figure 5.16. Experimental Velocity Profile as Function of Radial Distance in Liquid-Solid-Gas System with V_l=3.7 cm/sec and V_g=7.45 cm/sec

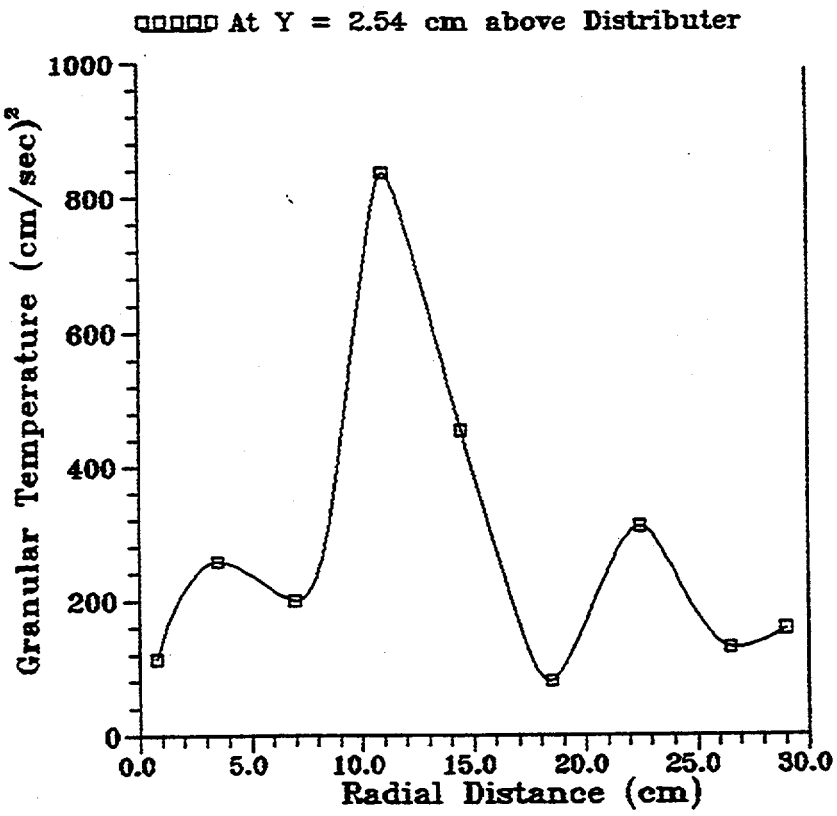

Figure 5.17. Solid Granular Temperature Vs. Radial Distance

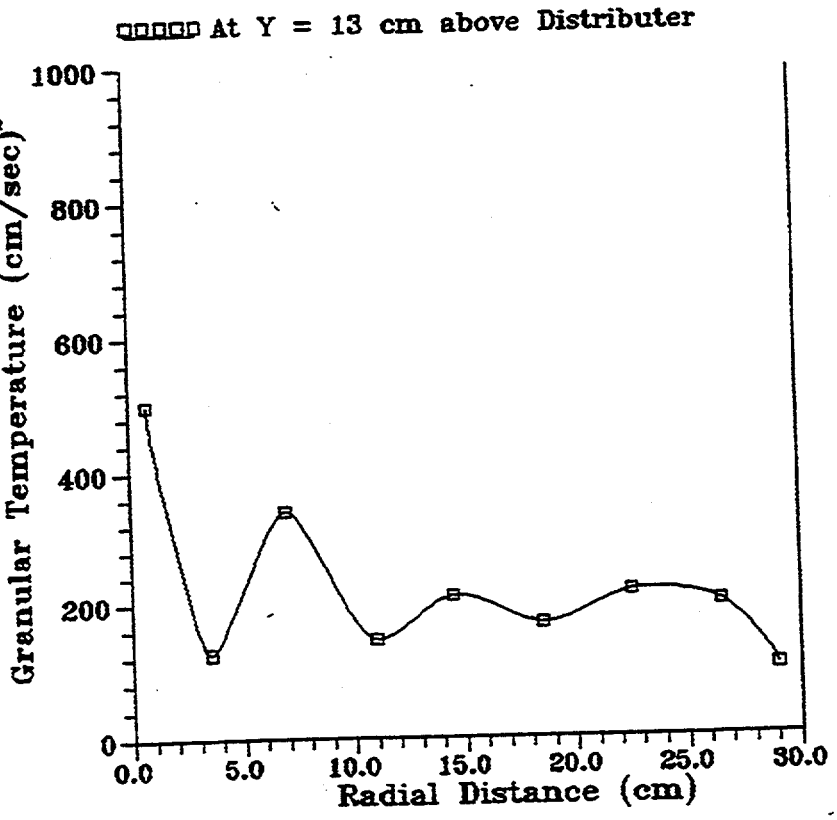

Figure 5.18. Solid Granular Temperature Vs. Radial Distance

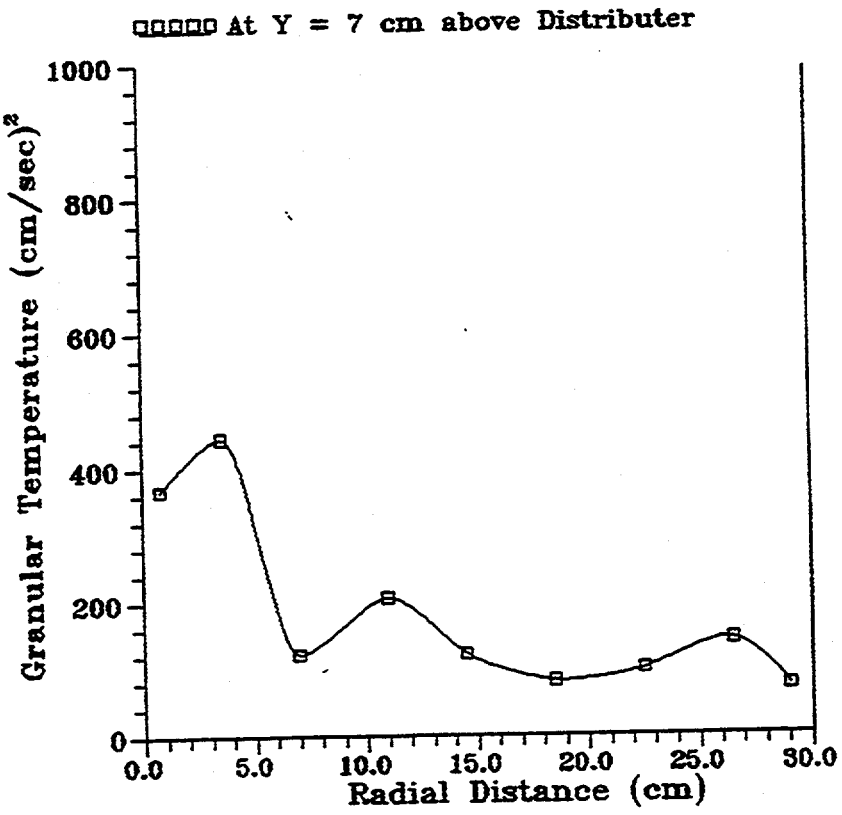

Figure 5.19. Solid Granular Temperature Vs. Radial Distance

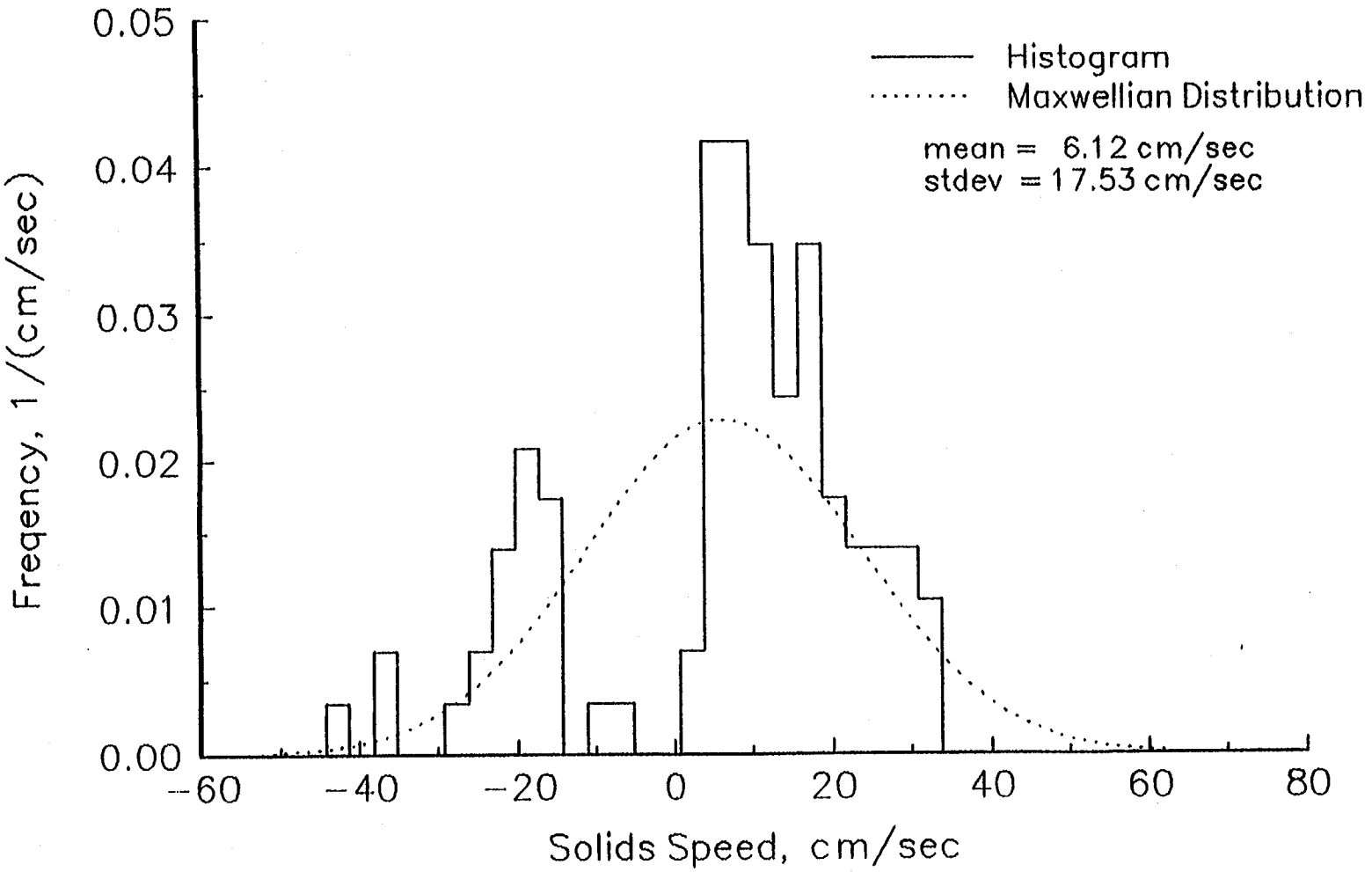

Figure 5.20. Distribution of Mean Solid Speed at X=23 cm and Y=10 cm for Liquid-Solid-Gas System with V_l=439 cm/sec and V_g1=243 cm/sec V_g2=578 cm/sec V_g3=370 cm/sec

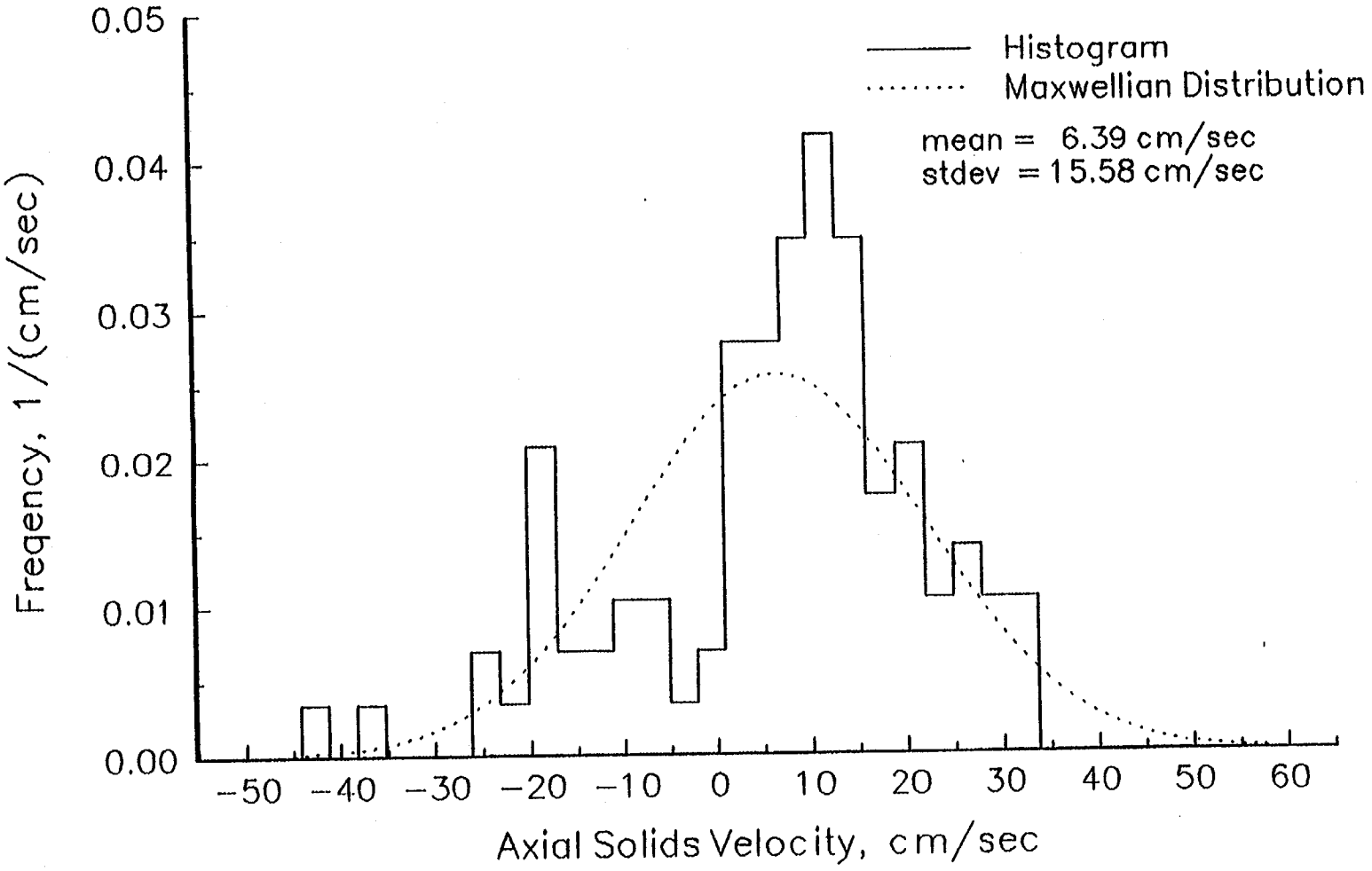

Figure 5.21. Distribution of Axial Velocity of Particles at X=23 cm and Y=10 cm for Liquid-Solid-Gas System with V_l=439 cm/sec and V_g1=243 cm/sec V_g2=578 cm/sec V_g3=370 cm/sec

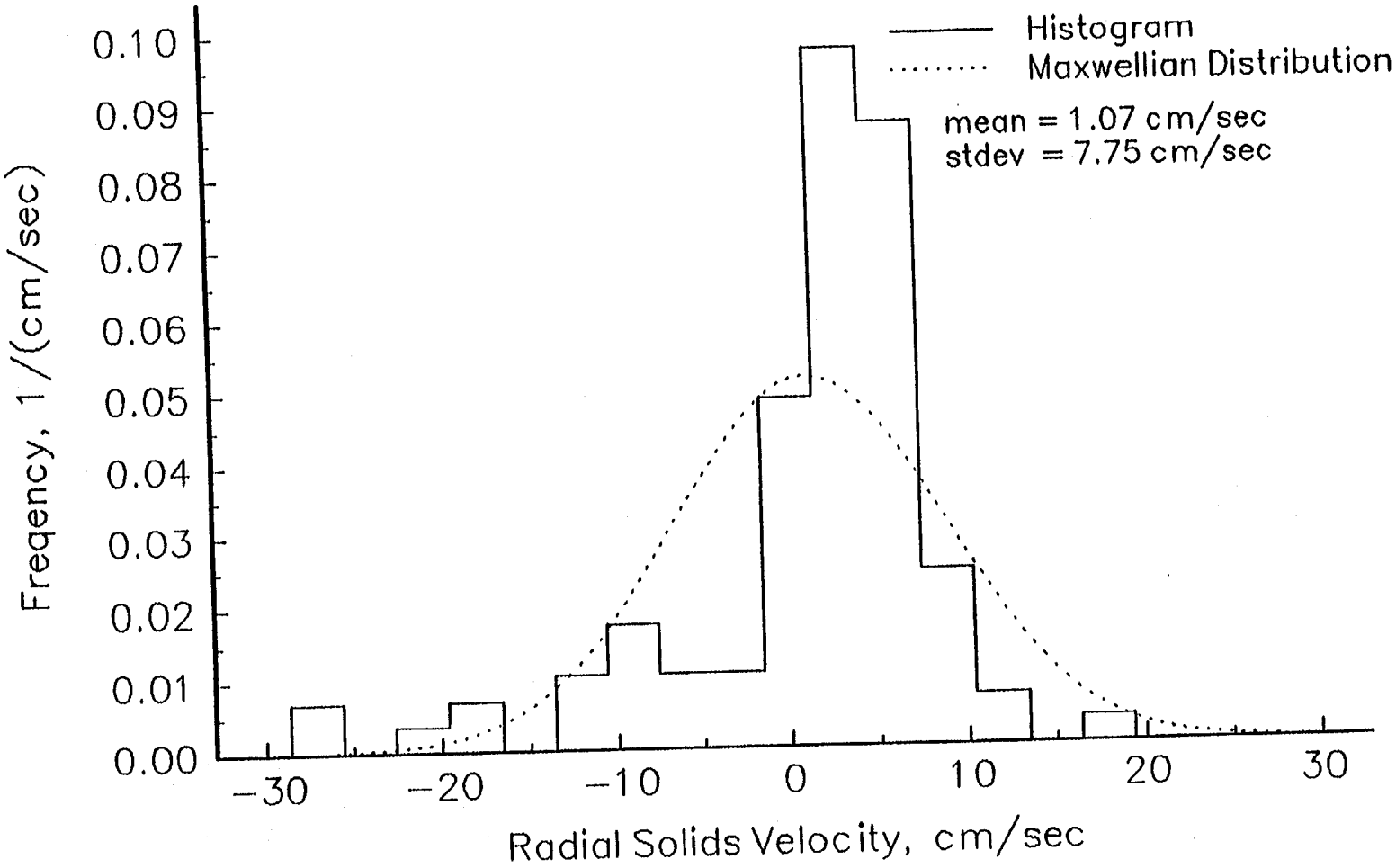

Figure 5.22. Distribution of Radial Velocity of Particles at X=23 cm and Y=10 cm for Liquid-Solid-Gas System with V_l=439 cm/sec and V_g1=243 cm/sec V_g2=578 cm/sec V_g3=370 cm/sec

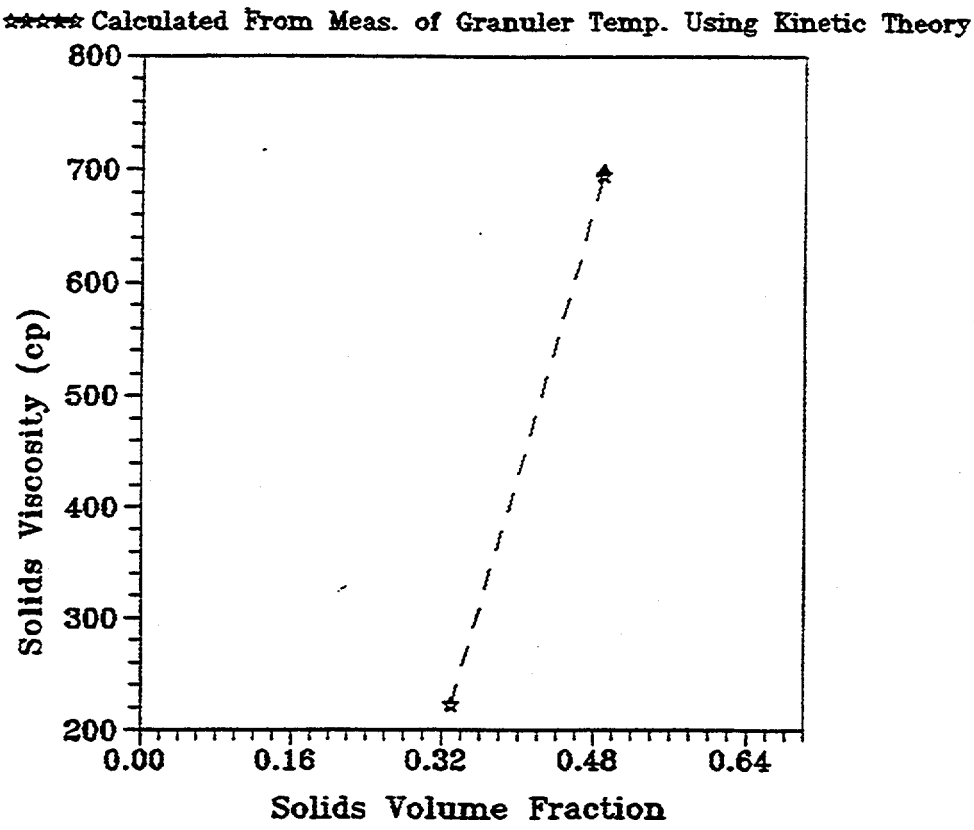

Figure 5.23. Solid Viscosity as Function of Liquid Velocity in Liquid-Solid-Gas Fluidized Bed with Central Jet Distributer